I.J. Image, Graphics and Signal Processing, **2015, 9, 11-19**
Published Online August 2015 in MECS (http://www.mecs-press.org/)
DOI: 10.5815/ijigsp.2015.09.02

Automatic Detection of Surface Defects on Citrus Fruit based on Computer Vision Techniques

Mohana S.H., Prabhakar C.J.
Dept. of P.G Studies and Research in Computer Science, Kuvempu University, Shankaraghatta-577451, Shimoga, Karnataka, India
E-mail: mohana.sh43@gmail.com, psajjan@yahoo.com

Abstract**—**In this paper, we present computer vision based technique to detect surface defects of citrus fruits. The method begins with background removal using k-means clustering technique. Mean shift segmentation is used for fruit region segmentation. The candidate defects are detected using threshold based segmentation. In this stage, it is very difficult to differentiate stem-end from actual defects due to similarity in appearance. Therefore, we proposed a novel technique to differentiate stem-end from actual defects based on the shape features. We conducted experiments on our citrus data set captured in controlled environment. The experiment results demonstrate that our technique outperforms the existing techniques.

Index Terms**—**Citrus stem-end detection, Circle fitting, Mean shift segmentation.

I. INTRODUCTION

Fruits play an important role in providing food and nutritional security as well as sustainable income to farmers all over the world. Most of the fruit varieties have been selected from the naturally -occurring superior chance seedlings taking into their earliness or lateness and qualitative attributes. There are innumerable numbers of varieties in fruit crops out of which only a few happen to be of commercial importance. Different regions across the country have their own commercial varieties because of wide range of adaptability. Of the various hybrids assessed so far, only a few have been found to be promising. Citrus fruits are acidic fruits with high nutrition. Citrus fruits act as a fabulous source of vitamin C and provide a wide range of essential nutrients that are required for the body. There are many varieties of citrus fruits are grown such as clementine, leech, grapefruit, mandarin, tangerine, kumquat, minneola, tangelo, lemon, orange and pummelo etc.

The surface defect detection of fruits is a challenging task, which influences market value and consumer preferences to purchase fruits. The early detection of fruit surface defects is a significant task in packing houses because a defected fruits can spread the infection such as fungal growth, bruises to other fruits, which are packed in the batch. Bruises are one of the significant defects of fruits, which could be caused by mechanical damage during harvesting or insect bites or fungal growth. Some Agro-industries are using automated fruit grading system to decrease production costs and meanwhile to increase the quality to the production, which works based on parameters such as size, weight and skin defects. The defect detection of surface defects especially bruises on fruits still facing some difficulties, because of its lack of knowledge, i.e., training by the supervisors. Now a day's computer vision system is becoming popular in many fields in which fruits grading and sorting tasks are the subset of the applications, which are totally automated systems, i.e., with only less human intervention. Surface defects are of great concern for the farmers and also for vendors to grade the fruits according to their defects presented in the surface of the fruits. The defect or damage is usually occurred in citrus fruits due to various factors. The citrus fruits with bruise, fungal growth, rot, disease and other defects must be removed to prevent cross contamination, and it helps to reduce subsequent processing cost.

The automatic detection of surface defects in fruits presents different problems such as the need of inspecting the whole surface of the fruit. Hence we need to capture the image which covers the whole surface of the fruit by rotating the fruit in a particular angle. The discrimination among different types of defects and stem-end during post harvest inspection is increasingly significant in order to enhance the possibilities of market value of fruit according to their external quality. The fruits which are having uniform color made defect detection task very simpler and accurate. Fruits are belonging to the same variety can have different colors depending on the stage of maturity. One of the main problems arising from the analysis of fruits is the wide diversity of colors and textures. The color of the defects in some fruits can even be similar to the healthy skin color and it reduces the discrimination rate of fruit's defects and healthy skin.

In general, a desirable feature for the automatic defect detection task is the capability to deal with new unpredictable defects that may occur during production, i.e., defects may occur by different situations. To solve these problems, we need to develop an efficient algorithm that can overcome these limitations, and it is suitable for variety of defect detection tasks. In addition, real-time compliance is a significant issue so that the overall production can be inspected in on-line. Thus, the acceptance of the novel defect detection of fruits is based on the efficiency and cost for the system. In post-harvest inspection of citrus fruits, one desirable feature is the capability to deal with new types of samples very easily. This methodology is closely related with the problems found during the inspection task. Due to the large variety of textures and colors present in citrus fruits, inspection system needs frequent training to adjust the discrimination power to the features of each variety of fruit. If the variety is changes, then we need to retrain the system which is a time-consuming task, and also it increases the system cost. Therefore, unsupervised and easy-to-train systems are useful in these types of problems.

Many researchers have proposed their ideas to the field of fruit quality grading. We listed some of the techniques, which demonstrate how they have conducted the experiments, what are the challenges they have accomplished, and their techniques to the field of fruits grading. Jiangbo Li et al., [1] proposed an automatic detection of common surface defects of oranges based on the combination of lighting transform with image ratio method. They have used only the mean intensity of red and green channels, which is used for image ratio computation. Similarly, the big area with an elongated region removal (BER) algorithm is used to discriminate stem-ends with defected regions in which the global threshold value of 0.8 is used. Total 960 orange images were used in their experiment, in which the training phase consists of 240 images and 720 samples for testing. The drawback of this paper is that, it cannot sort the oranges according to the type of defects. They have manually marked the defected regions and stem-end. The overall defect detection rate of 93.1% is achieved from their approach.

D G Kim et al., [2] proposed an approach for classification of grapefruit peel diseases based on the analysis of color texture features. The RGB images of grapefruits are captured for normal and five common diseased peels. The input RGB image is transformed into HSI model. The 39 texture features are extracted from transformed Hue (H), Saturation (S) and Intensity (I) of the fruit region based on the spatial gray-level dependence co-occurrence matrices (SGDM) for each fruit. The discriminant features are selected based on stepwise discriminant analysis approach i.e. they used Statistical Analysis System (SAS) STEPDISC approach. The experiment is conducted on 180 grapefruits, which consist of 30 samples from each peel condition. The texture classification is performed based on SAS DISCRIM function. The 20 samples from each peel variety are used for training and remaining 10 samples is used for testing. The best classification accuracy of 96.7% results from the HSI_13 classification model and the I_11 classification model yields the poor classification accuracy of 81.7%. The average classification accuracy of 96% is achieved for grapefruit peel diseases. F L Garcia et al., [3] proposed an automatic detection of skin defects in citrus fruit approach based on the multivariate image analysis. A total of 120 citrus fruits are used in their experiment, which consists of four cultivars such as Clemenules, Marisol, fortune and Valencia (30 samples from each variety). The unfolding operation is performed on the RGB image, which separates each channel using the window size 3x3. The Eigen-space is obtained by applying PCA on the mean centered color spatial feature matrix. The Singular Value Decomposition (SVD) is used to extract information of the Eigen-space. They used T^2 statistics to detect the defective areas and to build the corresponding map of those defected regions. The overall defect detection rate of 91.5% is achieved for varieties of defected regions. Similarly, the classification results for all cultivar samples with defected regions achieved the result of 94.2%.

Jiangbo Li et al., [4] proposed an approach to detect the common defects of oranges using hyperspectral reflectance imaging. The images of wavelength ranging from 550nm and 900nm are used. The Principal Component (PC) images are created for the hyperspectral images of oranges. They selected optimal spectral wavebands such as 691 and 769nm from the visible spectra region in their experiment. Stem-end identification is performed based on the band ratio images such as R875/R691, and it is separated using global threshold value of 0.8 which is applied on the ratio image. Similarly, a global threshold of 0.23 is used for defects and healthy skin separation. Experiment is performed for 270 independent samples, which includes 240 samples are having defected skin and remaining 30 samples are having healthy skin. The performance is estimated by using two detection methods, i.e., first method is based on two band ratio and PCA using two bands, and second method consists of two band ratio images with PCA using six bands. The overall accuracy is 93.7% for first method and 91.5% for second method. J Qin et al., [5] proposed a detection of citrus canker based on hyperspectral reflectance imaging with spectral information divergence. Ruby-red grapefruits with normal and six different bruised skins are involved for their experiment. Defects and healthy skin discrimination are done using the Spectral information divergence (SID) classification approach. A total of 210 grapefruits are used for the experiment which includes 30 samples from each skin variety. The overall classification accuracy of 96.2% is achieved for the optimized threshold value of 0.008.

Jose J. Lopez et al., [6] proposed an approach of computer-based detection and classification of flaws in citrus fruits. A set of 150 oranges from two varieties such as navel-late and valencia-late are used for the experiments, they used eight varieties of defects are used for performance evaluation. The defect area is segmented based on the boundary detection approach with Sobel gradient mask. The RGB and HSV color space models are used for feature extraction. The five features such as mean, range, variance, skewness and kurtosis are extracted from each detected region of each color channel. They used three different feature combinations, which include first combination include mean and range features. The second combination consists of variance, skewness and kurtosis. For the final combination, all features are considered together. For k-NN classifier, k value is fixed as 6, and the feed forward back-propagation neural network with 15 inputs, 1 hidden layer with 10 nodes and 8 output nodes is used.

Blasco J. et al., [7] developed a computer vision approach to detect the peel defects in citrus based on means of a region oriented segmentation algorithm. The region based image segmentation approach is proposed based on unsupervised techniques, which is used to detecting the peel defects of citrus fruits. Total 635 fruits are used in their experiment, which consists of 356 oranges and 279 mandarins. The peer group filtering approach is used for smoothing the image and removing the noise. An iterative region growing and merging approach are used to segment the fruit image which partitions the fruit area into normal skin and defected skin. This approach does not distinguish between the stem and the defects. The defect detection results of the unsupervised segmentation algorithm yield 94.2% detection rate. J. Qin et al., [8] proposed a real time approach of citrus canker detection based on two-band spectral imaging system. A camera unit includes a beam-splitter with two band-pass filters with central wavelengths at 730 and 830 nm. Total 360 ruby-red grapefruits with normal, canker lesions and other peel diseases are used for the experiments. The image registration is performed in the first step, the band ratio image, i.e., R830/R730 was calculated based on the registered images. Threshold based segmentation is used to separate canker lesion from the normal skin of the grapefruit. The decision is made based on the results of the image-processing steps, which includes two decisions such as fruit 'Canker' and 'No Canker'. After that, 'Canker' class is divided into three subclasses such as 'Grade1', 'Grade2' and 'Juice'. They are not considered whole grapefruit surface, which leads to a weak acceptance ratio by the consumers. They achieved overall accuracy of 95.3% for discriminating healthy skin with defected parts of the citrus.

Gomez Sanchis J. et al., [9] proposed a hyperspectral system for rottenness detection caused by Penicillium digitatum in mandarins. The hyperspectral imaging system for the range between 460 nm to 1020 nm is used for image acquisition. Total 200 mandarin fruits are selected and used in their experiment. Preprocessing step includes lighting correction based on white and dark reference images. They labeled 4 classes such as healthy skin, rotten skin, sporulated skin and stem, which represent the reference results for evaluation. From the whole dataset 40% of samples are used for training and remaining 60% samples is used for validation. Four feature selection methods such as correlation analysis, mutual information, stepwise multivariate regression and genetic algorithm are evaluated in order to select the most discriminant bands to separate rotten skin and healthy skin. Linear Discriminant Analysis (LDA) and Classification and Regression Trees (CART) are used for classification. The overall detection rate of 91% is achieved, which includes healthy skin and defected skin.

In this paper, we proposed a novel technique to detect the surface defects automatically. The main challenge involved in detection of surface defects is that due to similarity in appearance of stem-end and defects, existing algorithms identify stem-end part as an actual defect. This leads to poor performance of defects detection algorithms. Hence, we proposed method to discriminate the stem-end part with actual defects, which increases the accuracy of our algorithm. It is observed that, the shape of the stem-end is similar to circle shape where as surface defects are not in the form of circle shape and having an irregular shape. This characteristic motivated us to discriminate stem-end with defects based on circle shape. Since, the shape of the stem-end is equivalent to circle shape, we discriminate the stem-end from true defects by fitting circle on detected candidate objects. For stem-end region the circle covers the whole region where as for actual defects, it uncovers the part of the region. Based on this concept, we differentiate the stem-end part from actual defects.

The organization of the remaining section of the paper is as follows: In section II, description of our approach is demonstrated, which consists of the steps such as pre-processing, candidate objects detection and discrimination of stem-end with actual defects is demonstrated. Section III demonstrates the experimental results and discussion. Finally, Section IV draws the conclusion of this study.

II. Our Approach

In this paper, our main objective is to detect candidate objects and discriminate the stem-end from the actual defects of citrus fruits, which are presented on the fruit surface. The flow diagram of our approach is shown in the Fig. 1. The background removal and fruit area extraction is done using k-means clustering technique with hole filling operation. We adopted mean-shift segmentation algorithm for fruit region labeling [10]. For this labeled image, we applied multi-threshold based segmentation to detect the candidate objects which are present on the fruit surface. If there are no candidate objects found on the fruit surface, then we consider it as healthy fruit and further processing will not be done. If there are more than two candidate objects, we consider it as defected fruit, and it is directly rejected. If one or two candidate objects present on the fruit surface, then it is necessary to discriminate as stem-end or true defect. Because, between two candidate objects, there is chance of both may be true defects or one is stem-end, and another one are the true defect.

A. Preprocessing

The citrus fruit images are captured in a controlled environment with white background, which reduces the complexity of the background removal tasks from the captured images. The citrus images with a fixed image size of 256 x 256 are taken for experimentation purpose. In the first step, RGB image is converted into L*a*b* color space. The k-means clustering operation is performed on L*a*b* image and the result of k-means algorithm demonstrates that, the fruit area and background area is labeled by using two different colors, which helped us to discriminate the fruit area and background easily. Fig. 2 shows the background removal results of the original RGB fruit image. The k-means clustering separates the fruit region from the background with small holes present within the fruit region. These holes are removed using hole filling operation.

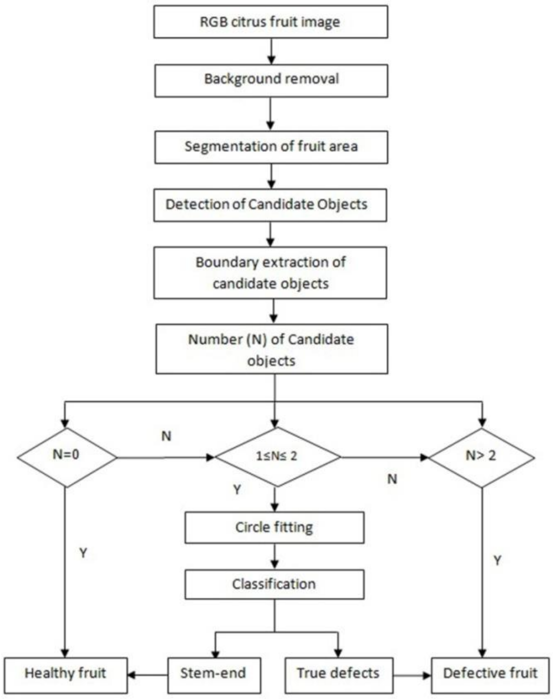

Fig.1. Flowchart of our approach

B. Candidate Objects Detection

We adopted Mean shift segmentation algorithm in order to label the fruit region and candidate objects are extracted from the fruit region by employing multi-threshold based segmentation. Mean shift approach is an old nonparametric density estimator proposed by Fukunaga and Hostetler in 1975 [11]. The image segmentation based on the mean shift algorithm is an extension of discontinuity preserving smoothing algorithm. An image may have different regions, and it is defined by all labeled pixels are associated with the same mode in the joint domain [10]. The mean shift segmentation is also known as a kernel based density estimation technique. This method is used to cluster an image by associating each pixel with a peak of the probability density. The peak in the local density is computed by first defining a window in the neighborhood of the pixel and afterwards calculating the mean of the pixels which lie within the window and then this window is shifted to the mean. The similar steps are repeated until the convergence. The mean shift vector is derived by estimating the density gradient of the image, and it indicates that the mean shift vector always points towards the direction of the maximum increase in density.

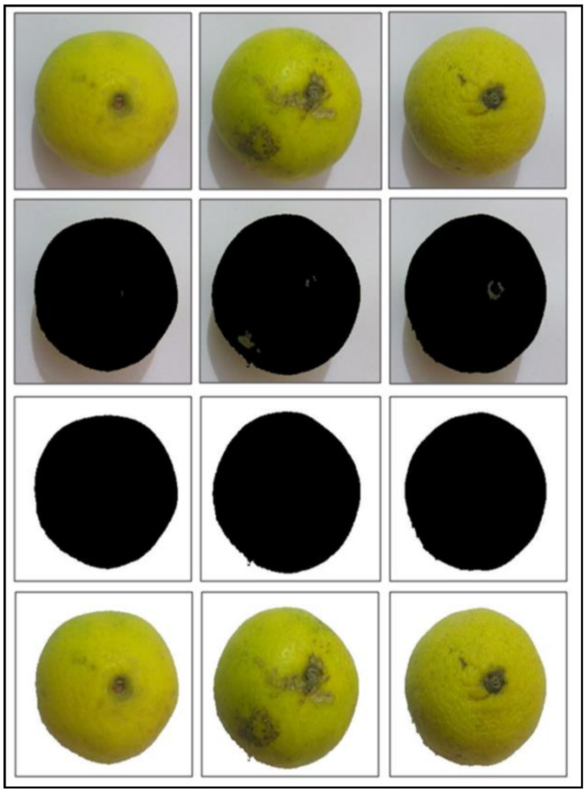

Fig.2. First row-Input citrus fruit images with stem-end and defects in view, Second row- Result of background removal using k-means clustering for the images shown in first row, Third row- After hole filling operation, Fourth row- Final result of background removal

In this mean shift segmentation, we used the spatial bandwidth of 16, range bandwidth of 8 and the minimum window size as 20 pixels i.e., $\left(h^s, h^r, M\right) = (16,8,20)$. The results of mean shift segmentation are shown in the Fig. 3. The mean shift segmentation result shows that, how the similar intensity is distributed in the image. Based on the intensity distribution, the similar intensity pixels are grouped each other. The mean intensity is estimated for each region, and this mean value is labeled for the whole region. From the mean shift segmented image of citrus fruit, it is observed that, candidate regions are labeled as isolated regions with uniform intensity values compared to the healthy region. Based on these labels, we can easily fix the threshold values for extraction of regions of candidate objects.

The citrus fruits are having variation in intensity values in both stem-end and defected regions. It is not easy to set only one threshold value for the threshold based segmentation operation in order to extract these regions. Hence, for threshold based segmentation, we considered three different threshold values such as 30, 50 and 70 based on the visual observation. The images are segmented several times at different threshold levels. Finally, the resultant images of multi-threshold segmentation are added to form a multi layer image. The resultant image demonstrates that, the candidate objects are having different color compared to the healthy region. The results obtained from the background subtraction and multi-threshold segmentation methods are mapped each other. The resultant image shows the candidate objects which are present on the citrus fruit surface. Finally, we extract the boundary (contour) of each candidate object using the canny edge detector. The Fig. 3 demonstrates that, the mean shift segmentation is applied to the result of preprocessed image. This result shows the result of multi-threshold segmentation, which yields contour of extracted candidate objects.

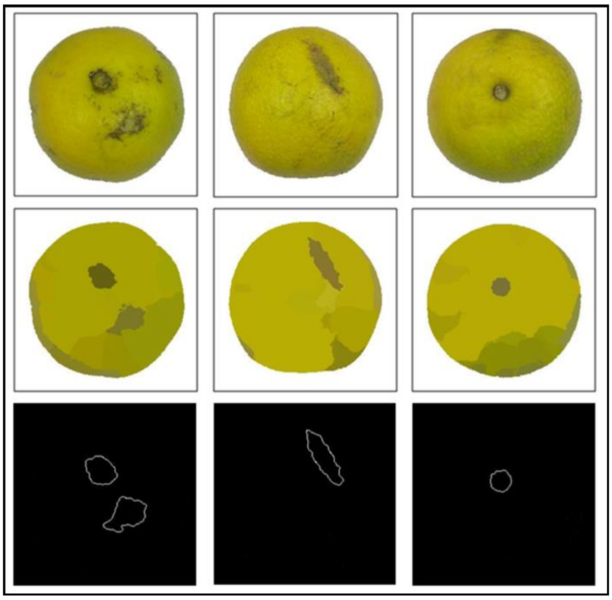

Fig.3. First row- Input images, Second row- mean shift segmentation results of first row images, Third row- Contour of the candidate objects

C. Discrimination of Stem-end and Actual Defects

The stem-end size of citrus fruit may vary during different cultivar and stages of the fruit growth. However, it does not vary in its shape i.e. it is almost similar to circle shape. Based on this characteristic, we detect and discriminate the stem-end from true defects by fitting the circle on each extracted candidate objects. In case of stem-end region, the circle encompasses the whole region of the candidate object where as for actual defect, it does not encompass the whole region because of irregular shape in nature. We measure the distance between the contour of the candidate object and fitted circle boundary in four directions such as top, bottom, left and right. If the measured distance lies within the threshold, then it is a stem-end region otherwise, it is a true defect. The Fig. 5 shows the circle fitting on each candidate object.

In the circle fitting approach, In order to fit the circle within the candidate object region, we need to find Center point, which is maximum distance from the contour of the candidate object. Because our main objective is to fit a circle which tries to cover the whole region within the candidate object, and also it must cover the maximum region of the candidate object. Hence, we employ the distance transform for the whole fruit region of the image and computed the distance between candidate object contour pixels and all other pixels, including candidate region pixels. This demonstrates that, how far the pixels are located from the contour of the candidate object. Based on the values computed for each pixel using distance transform, we select the point within the candidate object region as Center point, which yields maximum distance from the candidate object contour. Based on this center point, we plot the circle within that candidate object region with a radius (r_c) is equal to the distance between Center point and contour of the candidate object. After fitting the circle within the candidate object region, the region which is uncovered is calculated through estimating the distance between contour of the fitted circle and candidate object contour using the pixel difference technique in four directions such as top, bottom, left and right.

For each direction, we computed three distances, totally, we compute 12 distances in all four directions. These are denoted as $(d_1, d_2, ..., d_{12})$. The center of the circle is denoted as $C_{xy} = (C_x, C_y)$.

4	3	3	3	3	3	3	3	3	3	3	3
3	3	2	2	2	2	2	2	2	2	2	2
2	2	2	1	1	1	1	1	1	1	1	1
2	1	1	1	0	0	0	0	0	0	0	1
2	1	0	0	0	1	1	1	1	1	0	1
1	1	0	1	1	1	2	1	1	1	0	1
1	0	1	1	2	2	2	1	0	0	1	2
1	0	1	1	2	2	1	1	0	1	1	2
1	0	0	1	1	1	1	0	0	1	2	2
1	1	0	0	0	0	1	0	1	1	2	3
2	1	1	1	1	0	0	0	1	2	2	3
2	2	2	2	1	1	1	1	1	2	3	3

Fig.4. Demonstration of distance transform for the candidate object

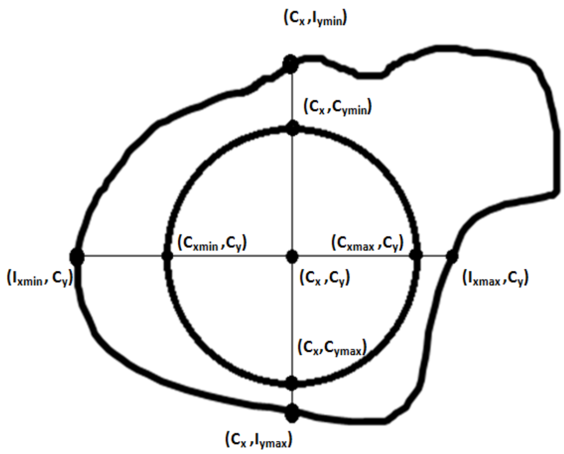

Fig.5. Graphical representation of circle fitted within the candidate object region

The distance measures such as d_1, d_2, d_3 *and* d_4 are calculated as follows:

$$d_1 = abs\left[\left(C_x, C_{y\min}\right) - \left(C_x, I_{y\min}\right)\right] \quad (1)$$

$$d_2 = abs\left[\left(C_x, C_{y\max}\right) - \left(C_x, I_{ymax}\right)\right] \quad (2)$$

$$d_3 = abs\left[\left(C_{x\min}, C_y\right) - \left(I_{x\min}, C_y\right)\right] \quad (3)$$

$$d_4 = abs\left[\left(C_{x\max}, C_y\right) - \left(I_{x\max}, C_y\right)\right] \quad (4)$$

In order to estimate d_9 *and* d_{11} along the horizontal axis of the upper part of the circle through the mid-point mp_1. This is calculated using the formula defined as

$$mp_1 = abs\left[round\left[\frac{\left(C_x, C_y\right) - \left(C_x, C_{y\min}\right)}{2}\right]\right] \quad (5)$$

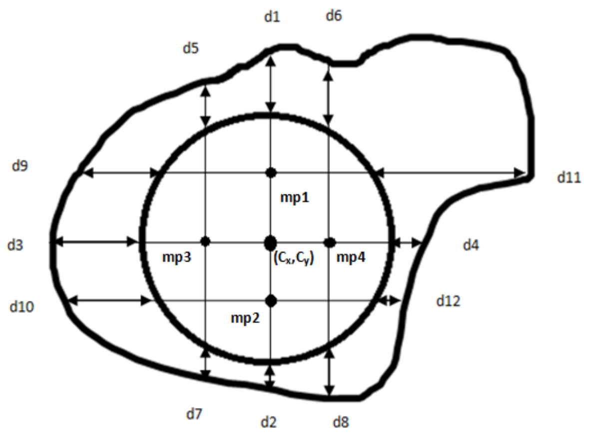

Fig.6. Graphical representation of various co-ordinates used to compute 12 distances

This midpoint divides the upper part of the circle equally in horizontal direction. We compute d_9 in the left side of the circle along the x-axis passes through the midpoint mp_1 as follows,

$$d_9 = abs\left[C_{x\min} - I_{x\min}\right], \quad (6)$$

where $C_{x\min}$ *and* $I_{x\min}$ are co-ordinate values of the pixels on the contour of the circle and candidate object respectively, along the x-axis passes through the midpoint mp_1.

Similarly, we compute d_{11} as follows,

$$d_{11} = abs\left[C_{x\max} - I_{x\max}\right], \quad (7)$$

where $C_{x\max}$ *and* $I_{x\max}$ are the co-ordinate values of the pixels on the contour of the circle and candidate object respectively, along the x-axis passes through the midpoint mp_1. Similarly, we compute the distances such as d_{10} *and* d_{12} using the mp_2 midpoint in lower portion of the circle, distances d_5 *and* d_7 using the mp_3 midpoint in lower left portion of the circle and distances d_6 *and* d_8 using the mp_4 midpoint in lower right portion of the circle. The location of these points and corresponding co-ordinates are shown graphically in the Fig. 6.

Fig.7. The result of circle fitting approach mapped on the candidate objects of mean shift segmented result

The distance between the circle fitted within the candidate object, and the contour of the candidate object is computed using 12 distances in all the four directions. The average of these 12 distances is estimated, and it is used for the discrimination task. Through several experiments conducted for various citrus fruit images, it is observed that the average of the 12 distances is less than or equal to 20 pixels for stem-end part and greater than 20 pixels for actual defect part. Based on this threshold value, we discriminate the stem-end part and actual defects.

III. Results and Discussion

Since there is no database, which contains images of defected citrus fruits, we created the database of citrus fruit images with healthy and defected fruits. The images are captured in a controlled environment, i.e., we placed a citrus fruit on a white background and with the uniform lighting system. We used the white background for citrus fruit acquisition, which reduces the complexity of the background removal. The citrus fruit images are captured with a fixed distance of 30cm between the camera and the background without any distortion. The image size is fixed with standard size of 256 x 256. We captured images of each fruit in four different views, which covers the whole fruit surface, and it helps to detect the defects. For experiment, we used 200 citrus fruits, totally, we captured 800 images (200 x 4 views), among which 400 images are healthy view, 120 images with stem-end in view, 80 images are with stem-end with one defect in view, and the remaining 200 images are having only actual defects in view. The actual healthy view, stem-end view, stem-end with one defect in view and defects in view are visually observed by human expert. The evaluation of the experimental results is carried out by comparing the experimental results with the human expert result.

We employed candidate objects extraction procedure as explained in the section 2.2. After extracted the candidate objects, the discrimination of stem end part from actual defects is not required for every test image. This is depending upon the number of candidate objects extracted from the fruit image. In the first case, if the fruit image does not contain/ contains more than two candidate objects, then we treat this fruit as healthy and defective fruit respectively. In this case discrimination of stem-end from the actual defects is not required, and it reduces the further processing time. In the second case, if the fruit image contains less than or equal to two candidate objects, then we need to perform discrimination of stem-end from actual defects. For this case, discrimination is done based on circle fitting approach for each candidate object. After fitting the circle on each candidate object region, we discriminate it as either stem-end or actual defect based on the amount of a region which is not covered by the circle measured in terms of pixel difference. As we explained, if the pixel difference lies within the threshold 20, then we treat the candidate object as stem-end part otherwise, it is an actual defect.

A. Uation for Circle Fitting Approach

The performance of circle fitting approach is evaluated using the Root Mean Square error (RMSE) of the Center point $\left(C_x, C_y\right)$ and radius $\left(r_c\right)$. The manually fitted circle is considered as ground truth, and it is used for the evaluation purpose. The variation in the center pixel co-ordinate of the ground truth circle with the center pixel co-ordinate of the circle fitted from our approach is considered as type-1 error. Similarly, the variation in the radius of the manually fitted circle with the circle fitted by our approach is considered as type-2 error.

We consider totally 280 candidate objects for evaluation purpose.

$$RMSE = \sqrt{\frac{\sum_{t=1}^{n}\left(y_t - y\right)^2}{n}} \tag{8}$$

where y_t is the predicted result of our approach, y is the actual result and n is the total number of predictions. In our case, n is the number of candidate objects.

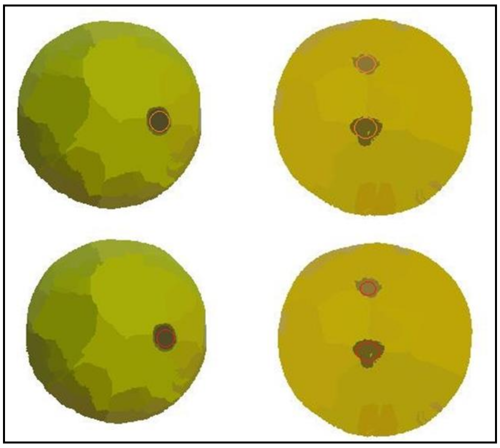

Fig.8. First row – Manually fitted circle within each candidate objects, Second row – Circle fitted by our approach

Table 1. Overall error rate of our approach

	Overall error rate
error in $\left(C_x, C_y\right)$	1.12
error in $\left(r_c\right)$	1.85

The evaluation of circle fitting approach is done based on the difference between the manually fitted circle within the each candidate object, and the circle fitted by our computer vision approach. The error rate is estimated with two different parameters, it consists of one is the center pixel coordinate and another one is the radius of the circle. These two types of errors are estimated for each candidate object, and the average error rate for center pixel and radius is shown in the Table 1.

B. Luation of Discrimination Approach

The experiment results of our approach are evaluated by comparing with actual results using the measures of Precision, Recall and F-score. Where tp (true positive) is the total number of actual stem end and actual defects are correctly detected as stem-end and defects respectively. The fp (false positive) is false detection result, i.e., total number of stem-end part is wrongly detected as actual defect and vice-versa. The Precision is defined as the ratio between the total number of correctly detected regions, and the total number of regions detected. Recall is the ratio of the number of correctly detected regions over the total number of actual defects. Recall is a measure of completeness, Precision is the measure of exactness, and F-score is a measure that combines precision and recall through their harmonic mean.

$$precision = \frac{tp}{tp + fp} \tag{9}$$

$$recall = \frac{tp}{tp + fn} \tag{10}$$

$$F - score = 2 * \frac{precision * recall}{precision + recall} \tag{11}$$

Table 2. Confusion matrix of citrus fruit stem-end and defects discrimination for our approach

	Healthy	Stem-end	Stem-end with one defect	Defects
Healthy	400	0	0	0
Stem-end	0	114	3	2
Stem-end with one defect	0	2	75	3
Defects	0	4	2	195
Total	**400**	**120**	**80**	**200**

Table 2 demonstrates the confusion matrix of our approach. From this table, we can observe that the healthy view is having total 400 samples, and all the samples are correctly detected as healthy view without any uncertainty. The stem-end view fruit samples are totally having 120 samples, among them 114 samples are correctly detected as stem-end view. The remaining 6 samples are wrongly detected as other categories. Total 80 samples are captured for stem-end with one defect in view. In which, 75 samples are correctly detected, and only 5 samples are not detected to the actual category. Similarly, 200 samples are having only defects in view. In which, 195 samples are correctly detected and remaining 5 samples is wrongly detected.

Table 3 demonstrates that, the accuracy of our approach in detection of defects and also the discrimination of stem-end with actual defects. The accuracy of healthy region is more accurately detected by our approach with 100% compared to the existing methods. Our approach achieves with an accuracy of 95.00% for stem-end region view, 93.75% for stem-end with one defected region view and 97.50% for actual defects view. The overall accuracy of 96.56% is obtained from our approach with low error rate. From these obtained results, we can observe that, our approach yields highest accuracy compared to the existing techniques.

The precision, recall and F-score are the measures used for the evaluation purpose. These precision and recall is measured based on the obtained results such as true positive, false positive and false negative. From Table 4, we can observe that, the precision and recall are almost nearest to the highest value, i.e., best result. The F-score is estimated based on the obtained precision and recall for each view of citrus fruit.

Table 3. Results of positive outcome and accuracy of our approach

Different views of citrus fruit	Total no. of actual results	Total no. positive outcome result	Total no. negative outcome result	Accuracy
Healthy	400	400	00	100%
Stem-end	120	114	06	95.00%
Stem-end with one defect	80	75	05	93.75%
Defects	200	195	05	97.50%

Table 4. Results of precision, recall and f-score achieved for our approach

Different views of citrus fruit	Precision	Recall	F-Score
Healthy	1	1	1
Stem-end	0.95	0.9579	0.95
Stem-end with one defect	0.9375	0.9375	0.93
Defects	0.975	0.9701	0.97

IV. Conclusion

In this paper, we proposed an approach to detect the citrus fruit defects and discrimination of stem-end part with actual defects is performed based on computer vision approach. The preprocessing step consists of background removal and fruit region extraction, it is performed using k-means clustering. The mean shift segmentation approach is used for citrus fruit region segmentation and multi-threshold based segmentation is used to detect the candidate objects. We extracted the contours of each candidate objects and the circle fitting approach is performed on each candidate objects. The distances between each candidate objects contour, and the circle fitted within that candidate objects is estimated. The extracted distance features are used to discriminate stem-end part with actual defects. The proposed approach yields an overall accuracy of 96.56% for citrus fruit defect detection. The proposed approach can be incorporated in citrus fruit grading technique as one of the steps in order to increase the citrus fruit grading accuracy.

References

[1] Jiangbo Li, Xiuqin Rao, Fujie Wang, Wei Wu and Yibin Ying. Automatic detection of common surface defects on oranges using combined lighting transform and image ratio methods. Postharvest Biology and Technology, Vol. 82, pages 59-69, 2013.

[2] Dae Gwan Kim, Thomas F. Burks, Jianwei Qin and Duke M. Bulanon. Classification of grapefruit peel diseases using color texture feature analysis. International Journal of Agricultural and Biological Engineering. Vol. 2, No. 3, pages 41-50, 2009.

[3] Fernando Lopez-Garcia, Gabriela Andreu-Garcia, Jose Blasco, Nuria Aleixos and Jose-Miguel Valiente. Automatic detection of skin defects in citrus fruits using a multivariate image analysis approach. Computers and Electronics in Agriculture, Vol. 71, pages 189-197, 2010.

[4] Jiangbo Li, Xiuqin Rao and Yibin Ying. Detection of common defects on oranges using hyperspectral reflectance imaging. Computers and Electronics in Agriculture, Vol. 78, pages 38-48, 2011.

[5] Jianwei Qin, Thomas F. Burks, Mark A. Ritenour and W. Gordon Bonn. Detection of citrus canker using hyperspectral reflectance imaging with spectral information divergence. Journal of Food Engineering. Vol. 93, pages 183-191, 2009.

[6] Jose J. Lopez, Maximo Cobos and Emanuel Aguilera. Computer based detection and classification of flaws in citrus fruits. Neural Computing and Applications, Vol. 20, No. 7, pages 975-981, 2011.

[7] Blasco J., Aleixos N. and Molto E. Computer vision detection of peel defects in citrus by means of a region oriented segmentation algorithm. Journal of Food Engineering, Vol. 81, pages 535-543, 2007.

[8] Jianwei Qin, Thomas F. Burks, Xuhui Zhao, Nikhil Niphadkar and Mark A. Ritenour. Development of a two-band spectral imaging system for real-time citrus canker detection. Journal of Food Engineering, Vol. 108, pages 87-93, 2012.

[9] Gomez-Sanchis J., Gomez-Chova L., Aleixos N., Camps-Calls G., Montesinos-Herrero C., Molto E. and Blasco J. Hyperscpectral system for early detection of rottenness

caused by Penicillium digitatum in mandarins. Journal of Food Engineering, Vol. 89, pages 80-86, 2008.

[10] Dorin Comaniciu and Peter Meer. Mean Shift: A Robust Approach Toward Feature Space Analysis. IEEE Transaction on Pattern Analysis and Machine Intelligence, Vol. 24, No. 5, pages 603-619, 2002.

[11] Fukunaga K. and L.D Hostetler. The Estimation of the Gradient of a Density Function, with Applications in Pattern Recognition. IEEE Trans. Information Theory, Vol. 21, pages. 32-40, 1975.

[12] Baohua Zhang, Wenqian Huang, Liang gong, Jiangbo Li, Chunjiang Zhao, Chengliang Liu and Danfeng Huang. Computer vision detection of defective apples using automatic lightness correction and weighted RVM classifier. Journal of Food Engineering, Vol. 146, pages 143-151, 2015.

[13] Wenqian Huang, Jiangbo Li, Qingyan Wang and Liping Chen. Development of a multispectral imaging system for online detection of bruises on apples. Journal of Food Engineering, Vol. 146, pages 62-71, 2015.

[14] Shimrat, M., "Algorithm 112: Position of point relative to polygon" 1962, Communications of the ACM Volume 5 Issue 8, Aug. 1962.

Authors' Profiles

Prabhakar C.J. received his Ph.D. degree in Computer Science and Technology from Gulbarga University, Gulbarga, Karnataka, India, in 2009. He is currently working as Assistant Professor in the department of Computer Science and M.C.A, Kuvempu University, Karnataka, India. His research interests are pattern recognition, computer vision, machine learning and video processing.

Mohana S.H. received his M.Sc. degree in Computer Science from Kuvempu University, Karnataka, India in 2010. He is currently pursuing his Ph.D. in Kuvempu University, Karnataka, India. His research interests are image processing, computer vision and machine vision.

How to cite this paper: Mohana S.H., Prabhakar C.J.,"Automatic Detection of Surface Defects on Citrus Fruit based on Computer Vision Techniques", IJIGSP, vol.7, no.9, pp.11-19, 2015.DOI: 10.5815/ijigsp.2015.09.02